Unsupervised Learning DOA Estimation aided by Array Imperfections Adaptive Filtering

Shuang Wu, Hongyu Pu, Taiyuan Luo

***Abstract*—In this paper, we present a novel method for estimating the Direction of Arrival (DOA) using adaptive filtering and unsupervised learning. The approach considers the impact of array imperfections on the accuracy of DOA estimation. Initially, we construct a spatial filter network trained on a limited set of available labeled data, allowing it to effectively handle complex nonlinear array imperfections. Next, We introduce MUSIC-NET, a method that maps the covariance matrix to spatial spectrum estimation through unsupervised learning utilizing synthetic data. This approach eliminates the need to estimate the number of sources and reduces reliance on labeled data. Our simulation results demonstrate that this innovative method successfully compensates for array imperfections, resulting in stable and reliable DOA estimates, even under conditions of low signal-to-noise ratios and limited snapshots. The accuracy of our estimations closely aligns with the Cramer-Rao Lower Bound (CRLB).**

***Index Terms*—Array imperfections, direction-of-arrival estimation, spatial filters, unsupervised learning**

I. Introduction

DIRECTION-of-arrival (DOA) estimation is widely used in radar, communication, sonar, and related fields [1]. Over the past few decades, numerous methods have been developed to address the DOA estimation challenge with super-resolution, high accuracy, and adaptability in low Signal-to-Noise Ratio (SNR) or small snapshot application scenarios [2], [3], [4], [5], [6], [7], [8]. For instance, the Multiple Signal Classification (MUSIC) [2] and Estimation of Signal Parameters via Rotational Invariance Technique (ESPRIT) [3] methods, which are based on the subspace orthogonality assumption, have achieved super-resolution direction finding at low SNR. Sparsity-inducing methods [9], [10], based on the over-complete steering matrix, accurately find direction using a single snapshot by reconstructing the spatial spectrum into a linear weighted representation of an over-complete basis. However, low-cost direction-finding systems often encounter complex array imperfections such as antenna position perturbations, mutual coupling effects, and gain/phase inconsistencies. These imperfections make it challenging to establish a mathematical model for the mapping from array output to signal direction, leading to a significant degradation in the performance of model-based methods [11].

Recent research has introduced deep learning techniques to tackle the DOA estimation challenge [12], [13], [14], [15], [16], [17], [18], [19]. These innovative methods do not depend on array geometry or calibration. Instead, they leverage a large training dataset with DOA labels to learn a probability distribution of signal directions to array outputs. This empowers the estimation of signal direction from the array output on test data, enhancing adaptability to array imperfections. One approach [20] involves a DOA estimation framework for supervised pre-training, which addresses array imperfections using a pre-trained autoencoder and then leverages a substantial amount of labeled data to establish the mapping of array output to signal direction. Another method [21] utilizes a significant amount of labeled data to model the signal subspace and address array imperfections, subsequently enabling accurate DOA estimation through spatial spectrum calculation. The difficulty of obtaining a significant amount of manually labeled data has prompted researchers, such as [22] and [23], to propose the development of a beamforming fitting loss function with sparse weighting constraints. This innovative approach allows for the unsupervised training of the DOA estimation network, presenting a promising solution to the challenge of data acquisition for training.

In this paper, we present a novel framework for DOA estimation. The framework comprises two independent networks, adaptive spatial filters, and MUSIC-NET. Notably, the training of the two networks is conducted entirely independently. To train the adaptive filter, only a small amount of manually labeled data specific to each array is required. This facilitates effective correction of complex array imperfections and recovery of the covariance matrix with the Toeplitz structure in ideal conditions. As for the MUSIC-NET, we have designed a MUSIC spectrum fitting loss function. Subsequently, unsupervised training with synthetic data enables the mapping from the covariance matrix to the MUSIC spectrum. Ultimately, the two trained networks are connected in series to execute high-precision DOA estimation for imperfect arrays. The simulation results validate the efficacy of our proposed method and demonstrate the superior accuracy of the DOA estimation compared to the state-of-the-art methods.

II. Problem Formulation

Assuming that an ideal uniform linear array (ULA) of M antennas spaced at half wavelength d receives K far-field narrowband signals, the incident directions of the signals are $\theta_k, k = 1, ..., K$. The array output, sampled uniformly at N instants, is represented by $\boldsymbol{X} = [\boldsymbol{x}(t_1), \boldsymbol{x}(t_2), ..., \boldsymbol{x}(t_N)] \in \mathbb{C}^{M\times N}$, and the sampling instances t_n are

$$\boldsymbol{x}(t_n) = \boldsymbol{A}\boldsymbol{s}(t_n)+\boldsymbol{n}(t_n) = \sum\nolimits_{k=1}^{K} \boldsymbol{a}(\theta_k)s_k(t_n) + \boldsymbol{n}(t_n) \quad (1)$$

The authors are with the Chengdu Fluid Power Innovation Center, China Aerodynamic Research and Development Center, Chengdu 610000, China (e-mail: wushuang@cardc.cn; 11539567@qq.com; 546928120@qq.com).

where $\boldsymbol{a}(\theta_k) = [1, ..., e^{-j2\pi(M-1)d\sin(\theta_k)/\lambda}]^{\mathrm{T}}$ represents the steering vector of the kth signal, while the vector $\boldsymbol{n}(t_n) = [n_1(t_n), n_2(t_n), ..., n_M(t_n)]^{\mathrm{T}}$ denotes the sampling vector of additive noise with a zero-mean Gaussian distribution. When considering a finite-length sampling of N instants, the array covariance matrix is denoted by

$$\boldsymbol{R} = \frac{1}{N}\sum_{i=1}^{N} \boldsymbol{x}(t_i)\boldsymbol{x}(t_i)^{\mathrm{H}} = \boldsymbol{U}_{\mathrm{s}}\boldsymbol{\Sigma}_{\mathrm{s}}\boldsymbol{U}_{\mathrm{s}}^{\mathrm{H}} + \boldsymbol{U}_{\mathrm{n}}\boldsymbol{\Sigma}_{\mathrm{n}}\boldsymbol{U}_{\mathrm{n}}^{\mathrm{H}} \quad (2)$$

where $\boldsymbol{\Sigma}_{\mathrm{s}} \in \mathbb{R}^{K\times K}$ and $\boldsymbol{\Sigma}_{\mathrm{n}} \in \mathbb{R}^{(M-K)\times(M-K)}$ are the signal eigensubspace corresponding to K large eigenvalues and the noise eigensubspace corresponding to $M-K$ small eigenvalues, respectively. As $N \to \infty$, the signal subspace becomes completely orthogonal to the subspace spanned by the steering vector, i.e

$$\boldsymbol{a}^{\mathrm{H}}(\theta_k)\boldsymbol{U}_{\mathrm{n}} \approx 0, k = 1, ..., K \quad (3)$$

In many academic studies on the DOA estimation, the MUSIC spectrum function is denoted as

$$\boldsymbol{p}_{\mathrm{MU}}(\theta) = \frac{1}{\boldsymbol{a}^{\mathrm{H}}(\theta)\boldsymbol{U}_{\mathrm{n}}\boldsymbol{U}_{\mathrm{n}}^{\mathrm{H}}\boldsymbol{a}(\theta)} \quad (4)$$

The array model is typically assumed to be ideal, with no mutual coupling or position deviation of the antennas, and perfectly consistent amplitude and phase gains. However, in practical applications, various array imperfections result in the array steering function, denoted as

$$\begin{aligned} &\boldsymbol{a}_e(\theta) = \boldsymbol{G}(\theta) \times \boldsymbol{C}(\theta) \times \boldsymbol{a}(\theta, \boldsymbol{l}) \\ &\boldsymbol{G}(\theta) = diag(\boldsymbol{g}_a(\theta) * e^{j\boldsymbol{g}_p(\theta)}) \\ &\boldsymbol{C}(\theta) = \mathcal{T}(\boldsymbol{c}(\theta)) \end{aligned} \quad (5)$$

deviating from the ideal $\theta \mapsto \boldsymbol{a}(\theta)$. Where $\boldsymbol{g}_a(\theta)$ and $\boldsymbol{g}_p(\theta)$ represent the gain and phase response functions with respect to θ, respectively. $\boldsymbol{c}(\theta)$ denotes the mutual coupling function with respect to θ, and $\mathcal{T}(\bullet)$ is the Toeplitz operator that constructs a Toeplitz matrix using a column vector. $\boldsymbol{l}$ represents the array antenna position deviation vector. Furthermore, the array output sampling and its covariance matrix can be formulated as

$$\begin{aligned} &\boldsymbol{x}_e(t_n) = \textstyle\sum_{k=1}^{K} \boldsymbol{a}_e(\theta_k)s_k(t_n) + \boldsymbol{n}(t_n) \\ &\boldsymbol{R}_e = \tfrac{1}{N}\textstyle\sum_{i=1}^{N} \boldsymbol{x}_e(t_i)\boldsymbol{x}_e(t_i)^{\mathrm{H}} \end{aligned} \quad (6)$$

III. Proposed Estimator Framework

As shown in Fig. 1, the proposed DOA estimation framework comprises spatial filters and MUSIC-NET. The solid arrows represent feedforward computation, while the dashed arrows represent the loss function gradient backpropagation. The spatial filters and MUSIC-NET are two separate deep neural networks, and we will offer a detailed introduction to their mathematical models and training methods.

A. Spatial Filters

The spatial filters consist of 4 dense layers. The output of neurons in each layer undergoes non-linear processing through the Tanh activation function, defined as $\mathrm{Tanh}(x) = (e^x - e^{-x})/(e^x + e^{-x})$. The input to the spatial filters is the column-wise concatenation of the real and imaginary parts of the covariance vector, expressed as $\boldsymbol{y}_e = [real(\boldsymbol{r}_e^{\mathrm{T}}), imag(\boldsymbol{r}_e^{\mathrm{T}})]^{\mathrm{T}} \in \mathbb{R}^{H\times 1}$, where $\boldsymbol{r}_e = vec(\boldsymbol{R}_e) \in \mathbb{C}^{M^2\times 1}$. Here, $real(\bullet)$ and $imag(\bullet)$ denote the operations for obtaining the real and imaginary parts, respectively. $vec(\bullet)$ represents the matrix vectorization operation, and $H = 2M^2$ represents the spatial filters' input dimensions. The output of the spatial filter is the concatenation of N_{SF} spatial subregion filtering results, denoted as $\hat{\boldsymbol{y}} = [\hat{\boldsymbol{y}}_1^{\mathrm{T}}, \cdots, \hat{\boldsymbol{y}}_{N_{\mathrm{SF}}}^{\mathrm{T}}]^{\mathrm{T}} \in \mathbb{R}^{(H*N_{\mathrm{SF}})\times 1}$, where $\hat{\boldsymbol{y}}_i \in \mathbb{R}^{H\times 1}(i = 1, ..., N_{\mathrm{SF}})$ represents the filtering result of $\boldsymbol{y}_e$ by the ith spatial filter.

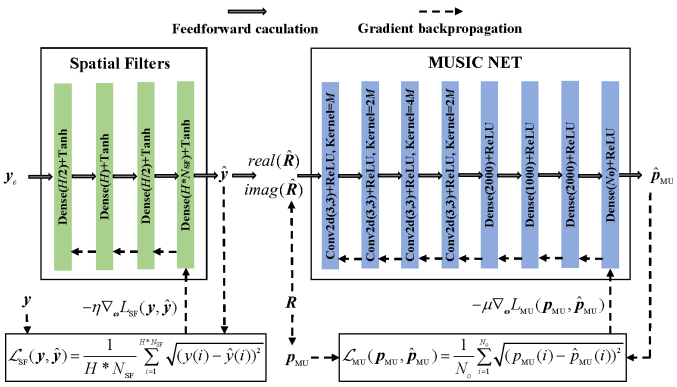

Fig. 1: The proposed estimator framework.

Consider the potential direction of the signal is $[\theta_{\min}, \theta_{\max}]$, which is uniformly sampled with an interval of $\Delta\theta$. The set of directions of the incident signal can be represented as

$$\boldsymbol{\Theta}_{\mathrm{SF}} = \{\theta_i | \theta_i = \theta_{\min} + (i-1)\Delta\theta, i = 1, ..., N_\theta\} \quad (7)$$

where $N_\theta = (\theta_{\max} - \theta_{\min})/\Delta\theta$. For each $\theta_i \in \Theta_{\mathrm{SF}}$, we collect $\boldsymbol{y}_e^i$ and $\boldsymbol{y}^i$ as the input of the spatial filter and the desired output, respectively, and then build the training set

$$\boldsymbol{\Omega}_{\mathrm{SF}} = \{(\boldsymbol{y}_e^i, \boldsymbol{y}^i) | i = 1, ..., N_\theta\} \quad (8)$$

We set N_{SF} spatial subregions in $[\theta_{\min}, \theta_{\max}]$, where each spatial subregion has a length of $L = N_\theta/N_{\mathrm{SF}}$ and $l = \lceil i/L \rceil$ denotes that θ_i is in the lth spatial subregion. For $j = 1, ..., N_{\mathrm{SF}}$, if $j = l$,

$$\begin{aligned} &\boldsymbol{y}_j(\theta_i) = [real(\boldsymbol{r}(\theta_i)^{\mathrm{T}}), [imag(\boldsymbol{r}(\theta_i))^{\mathrm{T}}]^{\mathrm{T}} \\ &\boldsymbol{r}(\theta_i) = vec(\boldsymbol{R}(\theta_i)) \end{aligned} \quad (9)$$

otherwise $\boldsymbol{y}_j(\theta_i) = \boldsymbol{0}$, and $\boldsymbol{y}^i = [\boldsymbol{y}_1^{\mathrm{T}}(\theta_i), \cdots, \boldsymbol{y}_{N_{\mathrm{SF}}}^{\mathrm{T}}(\theta_i)]^{\mathrm{T}}$.

In addition, we define the feedforward calculation of the spatial filters as $\hat{\boldsymbol{y}} = f_{\mathrm{SF}}(\boldsymbol{\omega}_{\mathrm{SF}}, \boldsymbol{y}_e)$, where $f_{\mathrm{SF}}(\bullet)$ represents the spatial filters model parameterized using the parameter set $\boldsymbol{\omega}_{\mathrm{SF}}$. The training of spatial filters can be formulated as a parameter optimization problem under the training set, represented as

$$\boldsymbol{\omega}_{\mathrm{SF}}^* = \arg\min_{\boldsymbol{\omega}_{\mathrm{SF}}}(\mathcal{L}_{\mathrm{SF}}(\boldsymbol{y}, \hat{\boldsymbol{y}})) \quad (10)$$

Here, $\mathcal{L}_{\mathrm{SF}}(\boldsymbol{y}, \hat{\boldsymbol{y}}) = \frac{1}{H*N_{\mathrm{SF}}} \sum_{i=1}^{H*N_{\mathrm{SF}}} \sqrt{(y(i) - \hat{y}(i))^2}$ denotes the loss function of the spatial filters. The gradient backpropagation of the loss function is represented as

$$\boldsymbol{\omega}_{\mathrm{SF}}^{new} = \boldsymbol{\omega}_{\mathrm{SF}}^{old} - \eta\nabla_{\boldsymbol{\omega}}\mathcal{L}_{\mathrm{SF}}(\boldsymbol{y}, \hat{\boldsymbol{y}}) \quad (11)$$

where $\boldsymbol{\omega}_{\mathrm{SF}}^{old}$ and $\boldsymbol{\omega}_{\mathrm{SF}}^{new}$ represent the current parameter set and the parameter set updated after one iteration, respectively. $\nabla_{\boldsymbol{\omega}}$ represents the gradient operation concerning the parameter set $\boldsymbol{\omega}$, and η represents the learning rate.

For the output of spatial filters, $\hat{\boldsymbol{y}} = [\hat{\boldsymbol{y}}_1^{\mathrm{T}}, ..., \hat{\boldsymbol{y}}_{N_{\mathrm{SF}}}^{\mathrm{T}}]^{\mathrm{T}}$, we reshape it into $[\hat{\boldsymbol{R}}_1, ..., \hat{\boldsymbol{R}}_{N_{\mathrm{SF}}}]^{\mathrm{T}}$, where $\hat{\boldsymbol{R}}_i, i = 1, ..., N_{\mathrm{SF}}$ denotes the filtering result of the ith spatial subregion. Finally, we calculate an estimate of the covariance matrix by summing over all filter outputs as

$$\hat{\boldsymbol{R}} = \sum_{i=1}^{N_{\mathrm{SF}}} \hat{\boldsymbol{R}}_i \tag{12}$$

B. MUSIC-NET

The proposed MUSIC-NET consists of 4 convolutional layers and 4 dense layers, with each layer's output being non-linearly processed by the ReLU activation function ($ReLU(x) = 0, x \leq 0$ or $x, x > 0$). The input of MUSIC-NET comprises two channels, namely $real(\hat{\boldsymbol{R}})$ and $imag(\hat{\boldsymbol{R}})$, while the output is denoted as $\hat{\boldsymbol{p}}_{\mathrm{MU}} \in \mathbb{R}^{N_o \times 1}$. When sampling $[\theta_{\min}, \theta_{\max}]$ uniformly by $\Delta\vartheta$, the output dimension of MUSIC-NET is $N_o = (\theta_{\max} - \theta_{\min})/\Delta\vartheta$.

First, we generate N_{train} training data using (2) and create the training set $\boldsymbol{\Omega}_{\mathrm{MU}} = \{\boldsymbol{R}^i | i = 1, ..., N_{\mathrm{train}}\}$. During the training process, we perform the calculation of $\boldsymbol{p}_{\mathrm{MU}}$ in parallel on the GPU following (4), which can be learned in detail from our code[1]. Additionally, we define the feedforward calculation of the MUSIC-NET as $\hat{\boldsymbol{p}}_{\mathrm{MU}} = f_{\mathrm{MU}}(\boldsymbol{\omega}_{\mathrm{MU}}, \boldsymbol{R})$, where $f_{\mathrm{MU}}(\bullet)$ represents the MUSIC-NET parameterized using parameter set $\boldsymbol{\omega}_{\mathrm{MU}}$. The MUSIC-NET training can be described as

$$\boldsymbol{\omega}_{\mathrm{MU}}^{*} = \arg\min_{\boldsymbol{\omega}_{\mathrm{MU}}} (\mathcal{L}_{\mathrm{MU}}(\boldsymbol{p}_{\mathrm{MU}}, \hat{\boldsymbol{p}}_{\mathrm{MU}})) \tag{13}$$

where $\mathcal{L}_{\mathrm{MU}}(\boldsymbol{p}_{\mathrm{MU}}, \hat{\boldsymbol{p}}_{\mathrm{MU}}) = \frac{1}{N_o} \sum_{i=1}^{N_o} \sqrt{(p_{\mathrm{MU}}(i) - \hat{p}_{\mathrm{MU}}(i))^2}$ denotes the loss function of the MUSIC-NET. The gradient backpropagation of the loss function can be formulated as

$$\boldsymbol{\omega}_{\mathrm{MU}}^{new} = \boldsymbol{\omega}_{\mathrm{MU}}^{old} - \mu \nabla_{\boldsymbol{\omega}} \mathcal{L}_{\mathrm{MU}}(\boldsymbol{p}_{\mathrm{MU}}, \hat{\boldsymbol{p}}_{\mathrm{MU}}) \tag{14}$$

where $\boldsymbol{\omega}_{\mathrm{MU}}^{old}$ and $\boldsymbol{\omega}_{\mathrm{MU}}^{new}$ represent the current parameter set and the parameter set updated after one iteration respectively. $\nabla_{\boldsymbol{\omega}}$ represents the gradient operation concerning the parameter set $\boldsymbol{\omega}$, and μ represents the learning rate.

In this paper, the MUSIC-NET is trained using synthetic data. For each synthesized $\boldsymbol{R}$, the source number K is known. During forward prediction, the MUSIC-NET produces a sparse spectrum output because of the ReLU function. The DOA estimates can be obtained by identifying peak locations on the smoothed spectrum, without requiring the source number prior.

IV. Simulations and Analyses

The simulation settings are outlined in Table 1. The spatial filters comprise $N_{\mathrm{SF}} = 6$ filters, with each covering a subregion of 20°. The spatial sampling is set with a spacing of $\Delta\theta = 1°$, resulting in a spatial grid of $\boldsymbol{\Theta}_{\mathrm{SF}} = \{-60° - 59°, ..., 59°\}$.

[1]The Source codes for this paper in Python can be found at https://github.com/wushuang-cardc/direction-of-arrival

A single training data with $SNR_{\mathrm{train}} = 10\mathrm{dB}$ is collected for each grid ($K_{\mathrm{train}} = 1$), resulting in a total of 120 training data for the spatial filters. To accommodate practical cases of array imperfections, we introduce a parameter $\rho \in [0, 1]$ to control the strength of imperfections and model the position deviation, gain deviation, phase deviation, and mutual coupling vector of the array antenna in a concise manner as

$$\boldsymbol{l} = \rho \times [\underbrace{-0.2, ..., -0.2}_{5}, \underbrace{0.2, ..., 0.2}_{4}]^{\mathrm{T}} \times d \tag{15}$$

$$\boldsymbol{g}_a(\theta) = \rho \times [0, \underbrace{0.2, ..., 0.2}_{5}, \underbrace{-0.2, ..., -0.2}_{4}]^{\mathrm{T}} \tag{16}$$

$$\boldsymbol{g}_p(\theta) = \rho \times [0, \underbrace{-30°, ..., -30°}_{5}, \underbrace{30°, ..., 30°}_{4}]^{\mathrm{T}} \tag{17}$$

$$\boldsymbol{c}(\theta) = \rho \times [0, \gamma^1, ..., \gamma^{M-1}]^{\mathrm{T}} \tag{18}$$

Where $\gamma = 0.3e^{j60°}$ is the mutual coupling coefficient between adjacent antennas. Then, in each training epoch, we randomly shuffle the training data and train $N_{epcoh} = 1000$ epochs with batch $N_{batch} = 64$ and learning rate $\eta = 10^{-3}$.

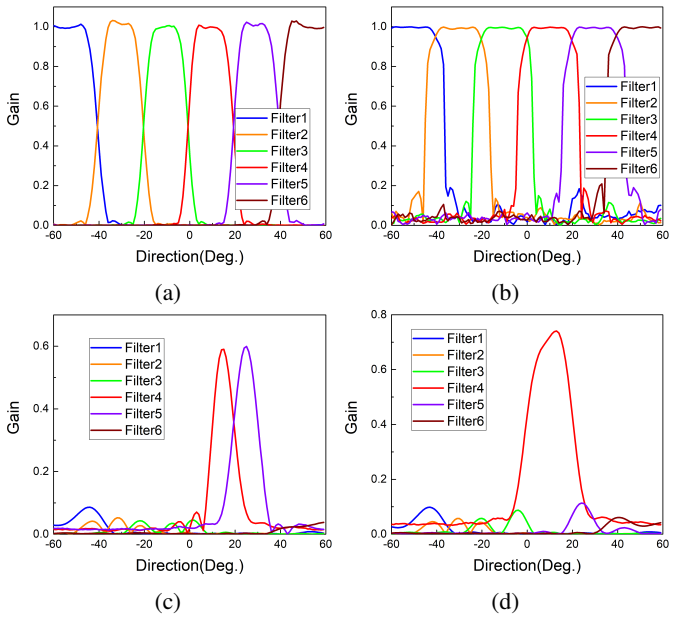

Fig. 2: The response of spatial filters. (a) Gain response $|\boldsymbol{y}_e^{\mathrm{H}}(\theta)\boldsymbol{y}_j(\theta)|$. (b) Phase response $\frac{|\boldsymbol{y}_e^{\mathrm{H}}(\theta)\boldsymbol{y}_j(\theta)|}{\|\boldsymbol{y}_e(\theta)\|_2 \|\boldsymbol{y}_j(\theta)\|_2}$. (c) The filtering result of two signals from direction $\theta_1 = 15°$ and $\theta_2 = 25°$. (d) The filtering result of two signals from direction $\theta_1 = 5°$ and $\theta_2 = 15°$.

TABLE I: Simulstion Settings

Array Parameters: $M = 10$, $N = 200$, $d/\lambda = 0.5$, $\theta_{\min} = -60°$, $\theta_{\max} = 60°$.
Spatial Filters: $N_{\mathrm{SF}} = 6$, $\Delta\theta = 1°$, $N_\theta = 120$, $\eta = 10^{-3}$, $K_{\mathrm{train}} = 1$, $SNR_{\mathrm{train}} = 10\mathrm{dB}$, $N_{epcoh} = 800$, $N_{batch} = 64$.
MUSIC-NET: $\Delta\vartheta = 0.1°$, $N_o = 1200$, $N_{\mathrm{train}} = 50000$, $K_{\mathrm{train}} = 2$, $SNR_{\mathrm{train}} \sim U(0\mathrm{dB}, 10\mathrm{dB})$, $\mu = 10^{-3}$, $N_{epcoh} = 50$, $N_{batch} = 2048$.

For MUSIC-NET, we use synthetic data for training and do not consider array imperfections. The spatial sampling is chosen as $\Delta\vartheta = 0.1°$, and the corresponding spatial grid is $\mathbf{\Theta}_{\mathrm{MU}} = \{-60° - 59.9°, ..., 59.9°\}$. We generate 50000 training data sets by randomly selecting the direction of two signals ($K_{\mathrm{train}} = 2$) from $\mathbf{\Theta}_{\mathrm{MU}}$ and setting $SNR_{\mathrm{train}} \sim U(0\mathrm{dB}, 10\mathrm{dB})$. Then, in each training epoch, we randomly shuffle the training data and train $N_{epcoh} = 50$ epochs with batch $N_{batch} = 2048$ and learning rate $\mu = 10^{-3}$.

After training the spatial filters and MUSIC-NET, we fixed their parameters. In the diagram shown in Fig. 2a and 2b, the spatial scope is evenly divided by multiple filters. Each filter bandwidth (3dB frequency point) perfectly corresponds to the boundary of the subregion. The flatness and linearity of the gain and phase responses within each filter bandwidth are satisfactory, indicating that the spatial filters can effectively filter out the nonlinear interference and noise superimposed on the input. Fig. 2c and 2d correspond to the scenario where two signals are incident from $\{15°, 25°\}$ and $\{5°, 15°\}$, respectively. This indicates that although the spatial filters is trained with one signal, its filtering performance is excellent in the case of two signals, even when the two signals are located in the same subregion.

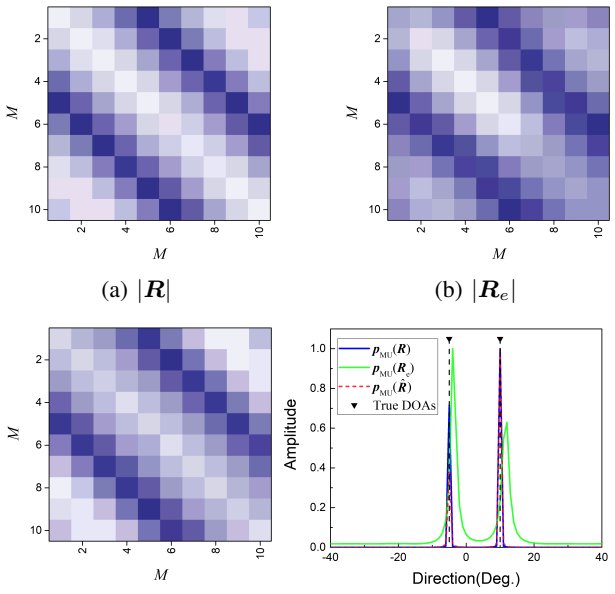

(a) $|\boldsymbol{R}|$ (b) $|\boldsymbol{R}_e|$

(c) $|\hat{\boldsymbol{R}}|$ (d) $\theta_1 = -5°, \theta_2 = 10°$.

Fig. 3: The spatial filters correction performance for array imperfections. (a) Ideal array. (b) Array imperfections without correction. (c) Array imperfections corrected by spatial filters. (d) Spatial spectrum of two signals.

Next, we designate the array imperfections strength parameter as $\rho = 0.2$. A comparison between Fig. 3a and 3b reveals that the Toeplitz structure of the covariance matrix is disrupted by array imperfections. However, our spatial filters effectively reconstruct the covariance matrix, as depicted in Fig. 3c. Furthermore, we validate this by presenting the MUSIC spectrum results in Fig. 3d.

As depicted in Fig. 4a, although MUSIC-NET utilizes 2 signals for unsupervised training, it can still accurately

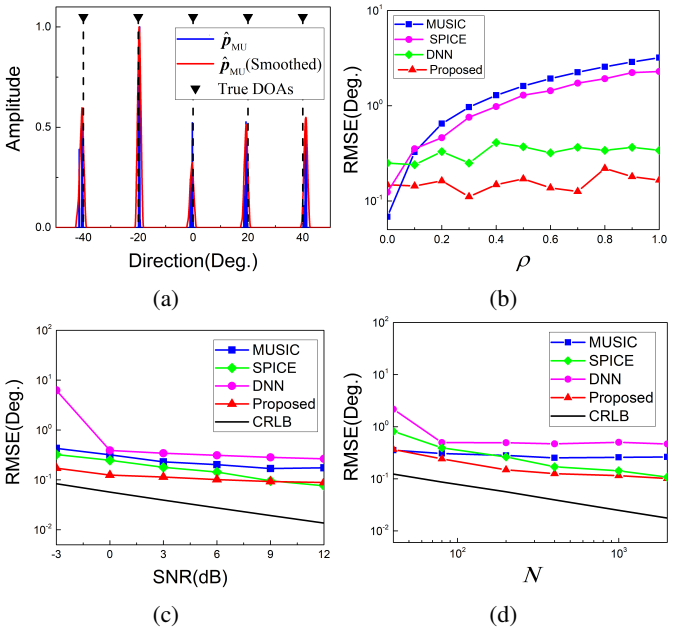

(a) (b) (c) (d)

Fig. 4: (a) 5 signals spatial spectrum of MUSIC-NET. (b) RMSE vs ρ. (c) RMSE vs SNR. (d) RMSE vs Snapshots.

estimate the DOA in a scenario involving 5 signals. Finally, we consider the proposed method's statistical performance. The Root Mean Square Error (RMSE) of DOA estimation is denoted as

$$RMSE = \sqrt{\frac{1}{N_{\mathrm{trail}} \times K} \sum_{n=1}^{N_{\mathrm{trail}}} \sum_{i=1}^{K} (\theta_i - \hat{\theta}_i)^2} \qquad (19)$$

where N_{trail} denotes the number of trials. In Fig. 4b, it is evident that as ρ increases, the performance of the MUSIC [2] and SPICE [10] degrades significantly. In contrast, the DNN in [20] and the proposed method show little sensitivity to array imperfections, with the proposed method demonstrating higher estimation accuracy than the DNN. Furthermore,, in Fig. 4c and 4d, it is demonstrated that the estimation error of the proposed method decreases with an increase in SNR or the number of snapshots. The estimation accuracy is closer to the CRLB [24] than other methods, indicating that the proposed method can better adapt to scenarios with low SNR and a small number of snapshots, and offers higher reliability and stability.

V. Conclusion

The proposed method for DOA estimation effectively addresses the impact of complex array imperfections by introducing the spatial filter. Our developed MUSIC-NET autonomously learns to extract angle features from the covariance matrix using synthetic data, which simplifies network training by replacing manual labels with the MUSIC spectrum. In comparison to state-of-the-art methods, our method demonstrates superior adaptability and stability in handling array imperfections, delivering excellent estimation performance even under low SNR and small snapshots, indicating promising practical applications.

REFERENCES

[1] H. Krim and M. Viberg, "Two decades of array signal processing research: the parametric approach," in *IEEE Signal Processing Magazine*, vol. 13, no. 4, pp. 67-94, July 1996, doi:10.1109/79.526899.

[2] R. Schmidt, "Multiple emitter location and signal parameter estimation," in *IEEE Transactions on Antennas and Propagation*, vol. 34, no. 3, pp. 276-280, March 1986, doi:10.1109/TAP.1986.1143830.

[3] R. Roy and T. Kailath, "ESPRIT-estimation of signal parameters via rotational invariance techniques," in *IEEE Transactions on Acoustics, Speech, and Signal Processing*, vol. 37, no. 7, pp. 984-995, July 1989, doi:10.1109/29.32276.

[4] D. Malioutov, M. Cetin and A. S. Willsky, "A sparse signal reconstruction perspective for source localization with sensor arrays," in *IEEE Transactions on Signal Processing*, vol. 53, no. 8, pp. 3010-3022, Aug. 2005, doi:10.1109/TSP.2005.850882.

[5] S. Chakrabarty and E. A. P. Habets, "Multi-Speaker DOA Estimation Using Deep Convolutional Networks Trained With Noise Signals," in *IEEE Journal of Selected Topics in Signal Processing*, vol. 13, no. 1, pp. 8-21, March 2019, doi:10.1109/JSTSP.2019.2901664.

[6] G. K. Papageorgiou, M. Sellathurai and Y. C. Eldar, "Deep Networks for Direction-of-Arrival Estimation in Low SNR," in *IEEE Transactions on Signal Processing*, vol. 69, pp. 3714-3729, 2021, doi:10.1109/TSP.2021.3089927.

[7] Y. Li and Y. Chi, "Off-the-Grid Line Spectrum Denoising and Estimation With Multiple Measurement Vectors," in *IEEE Transactions on Signal Processing*, vol. 64, no. 5, pp. 1257-1269, March1, 2016, doi:10.1109/TSP.2015.2496294.

[8] Z. Yang, L. Xie and C. Zhang, "A Discretization-Free Sparse and Parametric Approach for Linear Array Signal Processing," in *IEEE Transactions on Signal Processing*, vol. 62, no. 19, pp. 4959-4973, Oct.1, 2014, doi:10.1109/TSP.2014.2339792.

[9] Z. Yang, L. Xie and C. Zhang, "Off-Grid Direction of Arrival Estimation Using Sparse Bayesian Inference," in *IEEE Transactions on Signal Processing*, vol. 61, no. 1, pp. 38-43, Jan.1, 2013, doi:10.1109/TSP.2012.2222378.

[10] P. Stoica, P. Babu and J. Li, "SPICE: A Sparse Covariance-Based Estimation Method for Array Processing," in *IEEE Transactions on Signal Processing*, vol. 59, no. 2, pp. 629-638, Feb. 2011, doi:10.1109/TSP.2010.2090525.

[11] B. Liao and S. -C. Chan, "Direction finding in partly calibrated uniform linear arrays with unknown gains and phases," in *IEEE Transactions on Aerospace and Electronic Systems*, vol. 51, no. 1, pp. 217-227, January 2015, doi:10.1109/TAES.2014.130460.

[12] H. Huang, J. Yang, H. Huang, Y. Song and G. Gui, "Deep Learning for Super-Resolution Channel Estimation and DOA Estimation Based Massive MIMO System," in *IEEE Transactions on Vehicular Technology*, vol. 67, no. 9, pp. 8549-8560, Sept. 2018, doi:10.1109/TVT.2018.2851783.

[13] L. Wu, Z. -M. Liu and Z. -T. Huang, "Deep Convolution Network for Direction of Arrival Estimation With Sparse Prior," in *IEEE Signal Processing Letters*, vol. 26, no. 11, pp. 1688-1692, Nov. 2019, doi:10.1109/LSP.2019.2945115.

[14] Y. Guo, Z. Zhang, Y. Huang and P. Zhang, "DOA Estimation Method Based on Cascaded Neural Network for Two Closely Spaced Sources," in *IEEE Signal Processing Letters*, vol. 27, pp. 570-574, 2020, doi:10.1109/LSP.2020.2984914.

[15] D. T. Hoang and K. Lee, "Deep Learning-Aided Coherent Direction-of-Arrival Estimation With the FTMR Algorithm," in *IEEE Transactions on Signal Processing*, vol. 70, pp. 1118-1130, 2022, doi:10.1109/TSP.2022.3144033.

[16] X. Wu, X. Yang, X. Jia and F. Tian, "A Gridless DOA Estimation Method Based on Convolutional Neural Network With Toeplitz Prior," in *IEEE Signal Processing Letters*, vol. 29, pp. 1247-1251, 2022, doi:10.1109/LSP.2022.3176211.

[17] Z. -W. Tan, Y. Liu, A. W. H. Khong and A. H. T. Nguyen, "Gridless DOA Estimation Using Complex-Valued Convolutional Neural Network With Phasor Normalization," in *IEEE Signal Processing Letters*, vol. 30, pp. 813-817, 2023, doi:10.1109/LSP.2023.3292037.

[18] S. Feintuch, J. Tabrikian, I. Bilik and H. Permuter, "Neural-Network-Based DOA Estimation in the Presence of Non-Gaussian Interference," in *IEEE Transactions on Aerospace and Electronic Systems*, vol. 60, no. 1, pp. 119-132, Feb. 2024, doi:10.1109/TAES.2023.3268256.

[19] R. Cai and Q. Tian, "Two-Stage Deep Convolutional Neural Networks for DOA Estimation in Impulsive Noise," in *IEEE Transactions on Antennas and Propagation*, vol. 72, no. 2, pp. 2047-2051, Feb. 2024, doi:10.1109/TAP.2023.3332502.

[20] Z. -M. Liu, C. Zhang and P. S. Yu, "Direction-of-Arrival Estimation Based on Deep Neural Networks With Robustness to Array Imperfections," in *IEEE Transactions on Antennas and Propagation*, vol. 66, no. 12, pp. 7315-7327, Dec. 2018, doi:10.1109/TAP.2018.2874430.

[21] P. Chen, Z. Chen, L. Liu, Y. Chen and X. Wang, "SDOA-Net: An Efficient Deep-Learning-Based DOA Estimation Network for Imperfect Array," in *IEEE Transactions on Instrumentation and Measurement*, vol. 73, pp. 1-12, 2024, Art no. 8503512, doi:10.1109/TIM.2024.3391338.

[22] Y. Yuan, S. Wu, M. Wu and N. Yuan, "Unsupervised Learning Strategy for Direction-of-Arrival Estimation Network," in IEEE Signal Processing Letters, vol. 28, pp. 1450-1454, 2021, 10.1109/LSP.2021.3096117.

[23] Z. Zhang, X. Qu, W. Li, H. Miao and F. Liu, "DOA Estimation Method Based on Unsupervised Learning Network With Threshold Capon Spectrum Weighted Penalty," in *IEEE Signal Processing Letters*, vol. 31, pp. 701-705, 2024, doi:10.1109/LSP.2023.3349078.

[24] P. Stoica and A. Nehorai, "MUSIC, maximum likelihood, and Cramer-Rao bound," in *IEEE Transactions on Acoustics, Speech, and Signal Processing*, vol. 37, no. 5, pp. 720-741, May 1989, doi:10.1109/29.17564.